Bioorganic & Medicinal Chemistry 16 (2008) 10311–10318

Contents lists available at ScienceDirect

Bioorganic & Medicinal Chemistry

journal homepage: www.elsevier.com/locate/bmc

The importance of CH/π hydrogen bonds in rational drug design: An ab initio fragment molecular orbital study to leukocyte-specific protein tyrosine (LCK) kinase

Tomonaga Ozawa *, Eiichi Tsuji, Motoyasu Ozawa, Chiaki Handa, Harunobu Mukaiyama, Toshihiro Nishimura, Satoko Kobayashi, Kosuke Okazaki

Kissei Pharmaceutical Company Ltd., Central Research Laboratory, 4365-1 Kashiwabara, Hotaka, Azumino, Nagano-Pref 399-8304, Japan

ARTICLE INFO

Article history:
Received 29 August 2008
Revised 16 October 2008
Accepted 17 October 2008
Available online 22 October 2008

Keywords:
CH/π hydrogen bond
Weak hydrogen bond
An ab initio fragment molecular orbital method
Weak molecular interaction
Leukocyte-specific protein tyrosine (LCK) kinase
Rational drug design
Structure based drug design
Kinase inhibitor

ABSTRACT

The interaction energy was calculated, by the ab initio FMO method, for complexes between LCK protein and four inhibitors (staurosporine, BMS compound **2**, and our compounds **3** and **4**). In every case a number of CH/π hydrogen bonds have been disclosed in the so-called adenine pocket. In complexes of **2**, **3**, and **4**, CH/π and NH/π hydrogen bonds have been observed in another pocket. In view of the above results, the aniline ring of **3** was replaced by 2,6-dimethyl aniline to increase the potency for LCK kinase. A 10-fold increase in the potency has been achieved for **4** over **3**. We suggest that the concept of weak hydrogen bonds is useful in the rational design of drugs.

1. Introduction

Evidence has accumulated, in the preceding five decades, to show that weak molecular forces such as CH/O, NH/π, and CH/π hydrogen bonds are important in supramolecular chemistry and structural biology.[1,2] These weak hydrogen bonds have been shown to play an important role in the interaction of proteins with their specific ligands.[3,4] In view of the significance of CH/O hydrogen bonds in the recognition of proteins to their ligand,[5] Pierce et al. designed effective inhibitors of glycogen-synthase-kinase 3 (GSK3) by using the concept of the CH/O hydrogen bond.[6] Umezawa and Nishio reported that CH/π hydrogen bonds play a vital role in the binding of acetylcholine esterase with its inhibitors.[7] Irie also suggested the importance of CH/π hydrogen bonds in the binding of indolactam-V with C1B domain of protein kinase C.[8]

The ab initio MO method is rapidly becoming one of the most useful tools in studying interactions between molecules.[9–13] Kitaura and coworkers developed a technique termed as the ab initio fragment MO (FMO) method.[14–19] In the FMO method, a molecule or a cluster of molecules is divided into many fragments and the calculations are performed on each fragment and fragment pairs. The results obtained from the fragment pairs are combined and expressed as a summation of the fragment energies (inter-fragment interaction energies, IFIE). The IFIE value is used to estimate the interaction of a ligand with amino acid residues of a protein. The FMO technique has enabled the calculation of very large molecules including proteins and their complexes. The method has been extended to post-Hartree–Fock (HF) levels such as the second-order Möller–Plesset perturbation method (FMO-MP2).[20–22] The FMO-MP2 method is most often employed in the application to bio-macromolecules, because of its low computational costs. Fukuzawa and Nakano used the FMO method, at the MP2/6-31G* level, in evaluating the binding energy of a human-estrogen-receptor/ligand complex[23] and a cyclic-AMP receptor protein/DNA complex.[24] Nakanishi et al. applied the FMO method, at the MP2/6-31G* level approximation, to several complexes of FK506 binding protein (FKBP) and demonstrated that the dispersion interaction is important in binding FKBP with its specific ligands.[25] To evaluate the contribution from the CH/π hydrogen bond, MP2 or higher levels of theory should be used because the stabilization arises mostly from the dispersion force.[26] On the other hand, the electrostatic

* Corresponding author. Tel.: +81 263828820; fax: +81 263828827.
E-mail address: tomonaga_ozawa@pharm.kissei.co.jp (T. Ozawa).

0968-0896/$ - see front matter © 2008 Elsevier Ltd. All rights reserved.
doi:10.1016/j.bmc.2008.10.041

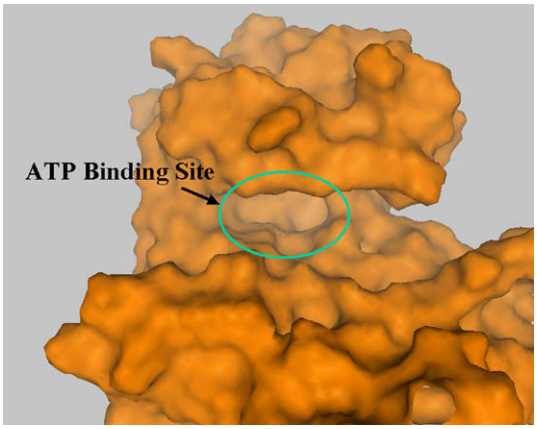

Figure 1. The ATP-binding site of the LCK protein kinase domain.

force determines the direction of interactions between interacting molecules.[27] Recently, we showed, by FMO calculations at the MP2/6-31G* level, that CH/π hydrogen bonds determine the selectivity of Src homology 2 domains to their ligand peptides.[28]

Src-family tyrosine kinases consist of eight highly homologous proteins that are expressed primarily in hematopoietic tissues,[29] two of which, LCK and FYN, are expressed in T cells, with LCK playing a critical role in the initial steps of T cell-receptor signaling.[30,31] Hence, an inhibitor of LCK has potential utility as an autoimmune agent. Several studies have reported on the synthesis and characterization of LCK kinase inhibitors.[32–43] These compounds are ATP-competitive inhibitors, and the crystal structure of various LCK complexes has been reported.[44] ATP is known to be bound in the cleft formed between the two lobes of the so-called protein kinase fold (Fig. 1).[45] Three sites that are common to all Src-family kinases are critical for the binding of LCK inhibitors (Fig. 2). Donor–acceptor pairs of hydrogen bonds are formed between the backbone atoms of the linker region and adenine. The adenine moiety is positioned at the so-called adenine pocket, which is composed mainly of aliphatic amino acid residues. Another pocket, which is unoccupied by ATP, binds an aromatic group of the inhibitors. Mukaiyama et al. proposed that CH/π hydrogen bonds play a role in the activity of the protein tyrosine kinase c-Src, and many aliphatic amino acid residues are found in the adenine and aromatic pockets of the enzyme.[46] Therefore, we hypothesized that electrostatic interactions and/or hydrogen bonds are relatively unimportant, while CH/π hydrogen bonds mainly contribute to recognition.

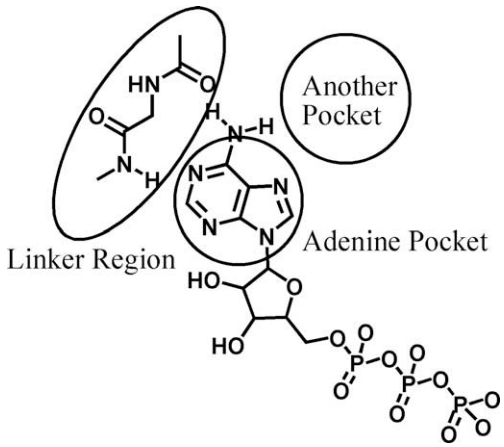

Figure 2. Features of the ATP-binding site.

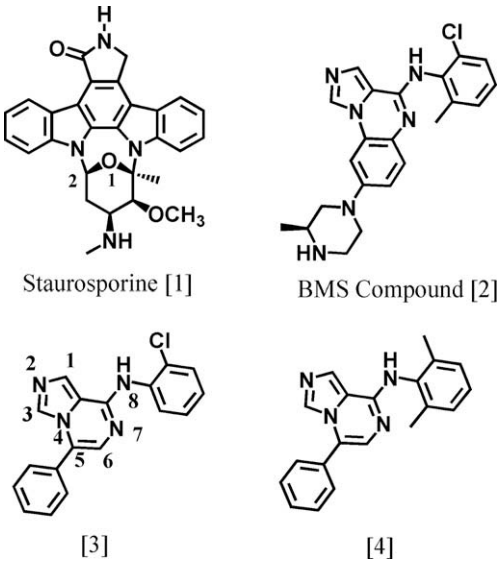

Figure 3. Structure of the four LCK inhibitors analyzed by the FMO method.

In view of the above information, a structure based drug design (SBDD) of LCK inhibitors was performed by crystal structure determinations and FMO calculations. Herein, we report the results of the FMO calculations of four complexes between LCK and inhibitors (Fig. 3). Several CH/π, CH/O, and NH/π hydrogen bonds have been found to contribute to stabilizing the structure of LCK complexes.

2. Results and discussion

2.1. Treatment of the dispersion interaction

Evaluating the interaction energies between the LCK protein and their inhibitors, analysis of the dispersion energy must be performed carefully. The electron correlation energy could be overestimated by MP2 calculations due to the lack of higher order correlations.

For estimating exactly the dispersion energy, a larger basis sets should be used. The 6-31G basis set was used throughout the present work, however, because we are dealing with a very large molecular system of ca. 4400 atoms (ca. 24,500 basis functions). The local MP2,[47] or spin-component scaled (SCS) MP2[48] are proposed as the method to improve the description of dispersion energy. Ishikawa et al., using the local MP2 method, showed that the ratio of dispersion interaction is not dependent on the size of basis sets, although the total dispersion interaction was greatly affected by the size of basis sets.[49] Therefore, the FMO/MP2/6-31G-level approximation was considered to be appropriate in discussing the tendency of the interaction between protein and ligand in rational drug design.

2.2. Staurosporine

Hydrogen bonds are formed in the linker region of the ATP-binding site of protein kinases, which is the key interaction in the recognition of inhibitors or substrates. Figure 4 illustrates the hydrogen bonds formed between staurosporine **1** and the enzyme. The crystal structure of the complex shows that the enzyme uses two hydrogen bonds.[44] One is found between the peptide oxygen of Glu317 and the lactam amide hydrogen of **1**. The other hydrogen bond is formed between the amide hydrogen of Met319 and the lactam carbonyl group of **1**. These two pairs of hydrogen bonds are important for the binding of the inhibitor to the protein kinase.

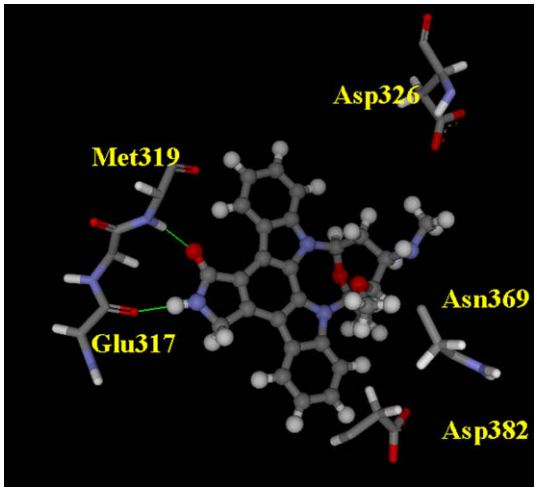

Figure 4. Interactions between **1** and Glu317 and Met319 of LCK. The green lines indicate hydrogen bonds.

Our FMO calculations gave results consistent with these observations. That is, the interaction energies E_{MP2} between **1** and the LCK protein have been estimated to be −19.4 and −11.0 kcal/mol, respectively, for Tyr#318 and Met#319. The interaction of Tyr#318 is reflected in the hydrogen bond between the peptide oxygen of Glu317 and **1**, according to the FMO fragment rule described in Section 4. Thus, the importance of the two hydrogen bonds between the linker region and **1** was confirmed by the FMO result.

The ATP-binding site also recognizes an aromatic group of the inhibitor. We investigated the mode of recognition by the FMO method. Table 1 shows that **1** interacts with Leu#251 (E_{MP2} −5.4 kcal/mol), Val#259 (−6.4 kcal/mol), and Leu#371 (−6.4 kcal/mol). No hydrogen bond was found between **1** and these three residues. The HF interaction energies E_{HF} were positive or slightly negative. These results imply that the contribution from the dispersion energy is important for the interaction involving these aliphatic residues: Leu#251 (E_{MP2-HF} −6.4 kcal/mol), Val#259 (−5.7 kcal/mol), and Leu#371 (−7.1 kcal/mol). Therefore, we consider that CH/π hydrogen bonds play a dominant role in the recognition of **1** by the LCK protein. In Figures 5 and 6, four short individual CH/π contacts were observed between Leu251, Val259, and Leu371 and **1**. Consequently, the FMO calculations suggest that the CH/π hydrogen bond plays an important role in the ATP site of the LCK protein. Crystal structures of several protein kinases revealed that the ATP-binding sites are similar to each other and occupied by an aromatic ring system of the inhibitor.[50]

Table 1
Interaction energies (in kcal/mol) between the LCK and staurosporine (**1**)

	E_{MP2}[a]	E_{HF}[b]	ΔE_{MP2-HF}[c]
Tyr318	−19.4	−13.6	−5.8
Asp382	−15.1	−11.2	−3.9
Gly252	−11.1	−6.9	−4.2
Met319	−11.0	−8.3	−2.7
Asn369	−10.9	−7.6	−3.2
Asp326	−8.3	−7.1	−1.1
Glu288	−7.4	−6.3	−1.1
Leu371	−6.4	0.7	−7.1
Val259	−6.4	−0.7	−5.7
Leu251	−5.4	1.0	−6.4
Lys269	−4.5	−4.5	0.0
Asp364	−4.2	−4.2	0.0
Gly254	−3.3	−2.8	−0.4
Thr316	−3.1	−1.6	−1.5
Val272	−3.0	−2.8	−0.2
Glu432	−2.1	−2.1	0.0
Asn321	−2.1	−1.8	−0.3
Gly322	−1.7	1.0	−2.8
Lys246	−1.7	−1.7	0.0
Gly262	−1.6	−1.6	0.0
Val372	−1.6	−1.4	−0.2
Asp422	−1.5	−1.5	0.0
His267	−1.1	−1.1	0.0
Lys379	−1.0	−1.0	0.0

[a] Interaction energy calculated at the MP2/6-31G level.
[b] Interaction energy calculated at the HF/6-31G level.
[c] $E_{MP2} - E_{HF}$.

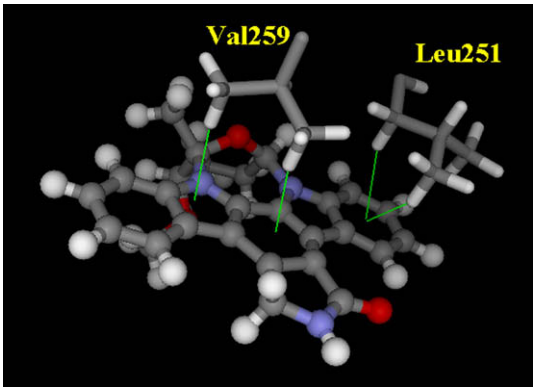

Figure 5. Interactions between **1** and Leu251 and Val259 of LCK. The green lines indicate CH/π hydrogen bonds.

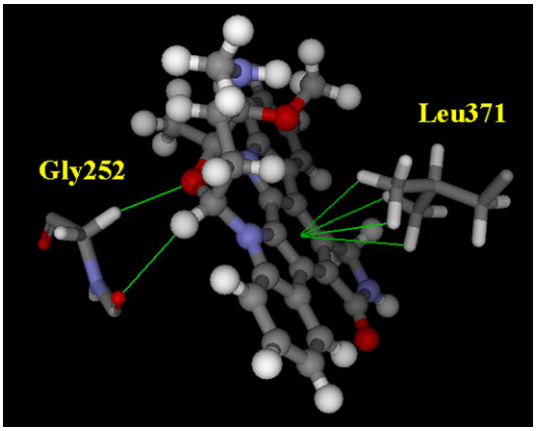

Figure 6. Interactions between **1** and Gly252 and Leu371 of LCK. The green lines indicate CH/O and CH/π hydrogen bonds.

The glycosyl part of **1** also interacts with the LCK protein. The crystal structure of the complex shows that the methylamino group of the glycosyl part of **1** is involved in a hydrogen bond with the LCK protein. This group is positioned to allow hydrogen bonding to a carbonyl group of the LCK protein. The FMO results gave results consistent with this; **1** interacts with Asp#382, Asn#369, and Asp#326 through electrostatic interactions and hydrogen bonds. The interaction between Gly#252 and the LCK protein is difficult to explain, but it may be due to CH/O hydrogen bonds between Cα of Gly252 and 1-oxygen of the glycosyl group, a carbonyl oxygen of Gly252, and a hydrogen attached to carbon-2 (Fig. 3).

The Mulliken charges were examined for several atoms. The atomic charges of the peptide oxygen of Glu317 and the lactam amide hydrogen of **1** are −0.702e and 0.468e, respectively. The amide hydrogen of Met319 and the lactam carbonyl oxygen of **1** are 0.498e and −0.709e, respectively. In contrast, the side chain hydrogen of Leu251, Val259, and Leu371, which are interacting

to aromatic ring of **1** through the CH/π hydrogen bonds, have charges 0.216e (Leu251 β position), 0.173e (Leu251 δ position), 0.210e, 0.173e (Val259 γ position), 0.166e, 0.165e, and 0.150e (Leu371 δ position), respectively. These results indicate that the electrostatic energy is relatively unimportant in the CH/π hydrogen bond.

To summarize this section, FMO calculations showed that the CH/π hydrogen bond, in addition to conventional hydrogen bonds and electrostatic interactions, is important in the recognition of the LCK protein to **1**. Therefore, the CH/π hydrogen bond, as well as the hydrogen bond, must be taken into account in the following drug design.

2.3. BMS compound

The Lipinski's 'rule-of-five' states that "to be a useful drug, at least five hydrogen bond donor- and 10-acceptor-functionalities should be achieved in a candidate molecule."[51] Recently, a 'rule-of-three,' which limits the number of hydrogen bond donors to three, has been proposed.[52] In BMS compound **2**, the number of hydrogen bond donors is smaller than in other kinase inhibitors.[40] The BMS compound was chosen as the lead compound of our study since this shows one CH/O hydrogen bond in the linker region of the LCK protein. Chen et al. reported that analogs of compound **2** have two hydrogen bonds that are critical in the binding of protein: N^3-nitrogen of the imidazole group to NH of Met319, and NH of the aniline moiety to OH of Thr316.[40] They, however, did not comment on the role of CH/O hydrogen bonds.

Table 2 shows that **2** interacts with Met#319, Tyr#318, and Thr#316, etc. (see Fig. 7). The interactions involving Met#319 correspond to those between the amide hydrogen of Met319 and N_3 of the imidazole part of **2**. Tyr#318 consists of the carbonyl group of Glu317, while Tyr318 does not include its carbonyl group. The crystal structure of the complex shows that the side chain of Tyr#318 is more than 4.2 Å from **2** (Fig. 8). We therefore consider that **2** interacts with Tyr#318 through a CH/O hydrogen bond.[53] The distance between the carbonyl group of Tyr#318 and the hydrogen attached to C4 of the imidazole ring was reported to be about 2.4 Å; this is compatible with the observation by Pierce et al., which mentioned the importance of CH/O hydrogen bonds in kinase inhibitors.[5,6]

Table 2
Interaction energies (in kcal/mol) between the LCK and BMS compound (**2**)

	E_{MP2}[a]	E_{HF}[b]	ΔE_{MP2-HF}[c]
Met319	−8.4	−5.2	−3.3
Tyr318	−8.2	−5.7	−2.5
Thr316	−7.3	−2.3	−5.0
Asp326	−7.0	−5.8	−1.3
Lys273	−7.0	−1.4	−5.7
Glu288	−5.1	−2.9	−2.2
Gly252	−5.1	−2.8	−2.3
Leu371	−4.3	0.2	−4.5
Val272	−3.3	−2.7	−0.6
Ile315	−3.3	−2.2	−1.1
Val259	−3.1	1.0	−4.1
Met292	−1.9	−0.6	−1.3
Leu251	−1.9	0.7	−2.6
Lys269	−1.5	−1.5	0.0
Phe383	−1.3	−0.3	−1.0
Trp260	−1.2	−0.9	−0.3
Lys379	−1.2	−1.2	0.0
Ile314	−1.2	0.4	−1.5
Leu303	−1.0	−1.0	0.0

[a] Interaction energy calculated at the MP2/6-31G level.
[b] Interaction energy calculated at the HF/6-31G level.
[c] $E_{MP2} - E_{HF}$.

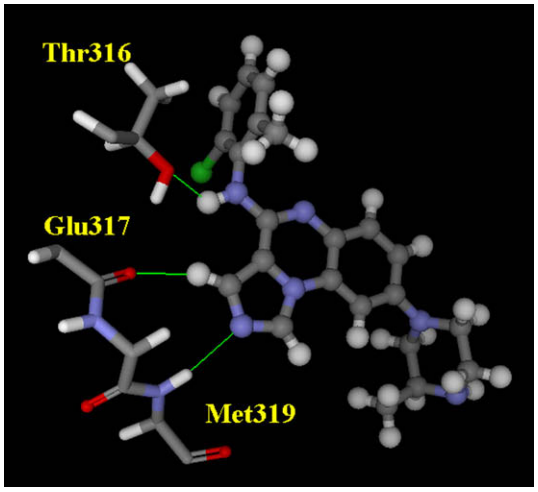

Figure 7. Interactions between **2** and Thr316, Glu317, and Met319 of LCK. The green lines indicate hydrogen bonds.

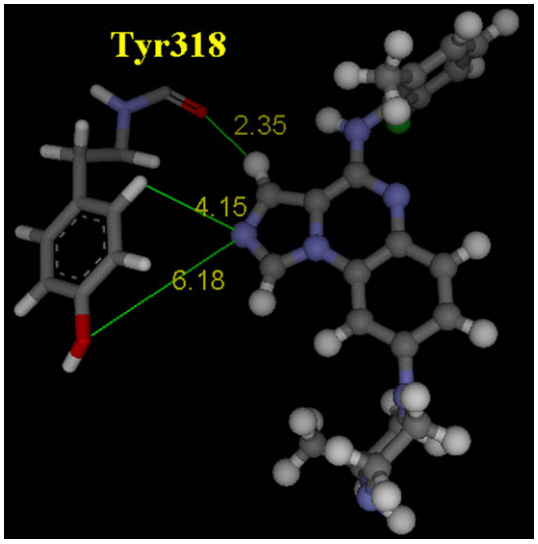

Figure 8. The distance between **2** and Tyr318.

The interactions involving Thr316 correspond to those between the hydroxyl group of Thr316 and the hydrogen of the aniline part. In the tricyclic aromatic part, several short CH/π distances have been disclosed (Fig. 9). Thus, Table 2 shows that **2** interacts with Leu251 (ΔE_{MP2} −1.9 kcal/mol), Val259 (−3.1 kcal/mol), and Leu371 (−4.3 kcal/mol). The above three residues have significant dispersion interactions: Leu251 (E_{MP2-HF} −2.6 kcal/mol), Val259 (−4.1 kcal/mol), and Leu371 (−4.5 kcal/mol). These interactions are weaker than those found in the **1**-complex. This is considered to be attributable to the difference in the number of CH/π hydrogen bonds.

We thought that the interaction energy involving the tricyclic aromatic portion would be adequate to be a candidate for the lead compound. In the 2-chloro-6-methyl-aniline part, short CH/π contacts were disclosed between the benzene ring and the side chain of Lys273 and Thr316. The interactions energies E_{MP2} were −7.0 kcal/mol for Lys273 and −7.3 kcal/mol for Thr316, while ΔE_{MP2-HF} was −5.7 kcal/mol and −5.0 kcal/mol, respectively, for Lys273 and Thr316. The ε-amino group of Lys273 was located above the benzene ring of 2, which may have been due to a NH/π hydrogen bond.

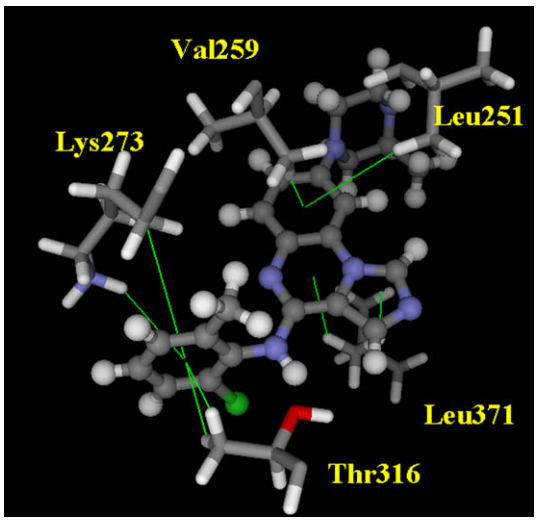

Figure 9. Interactions between **2** and Leu251, Val259, Lys273, Thr316, and Leu371 of LCK. The green lines indicate NH/π and CH/π hydrogen bonds.

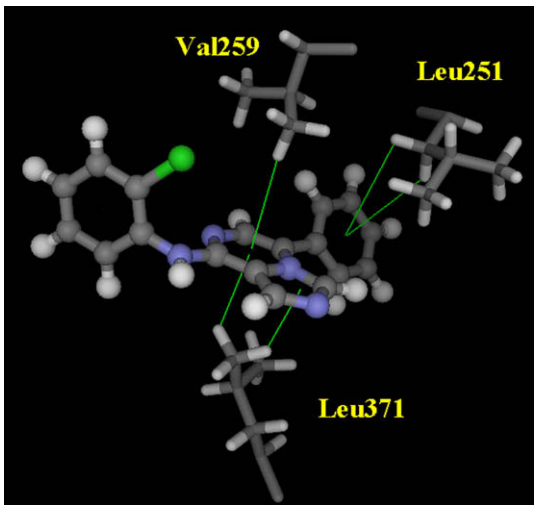

Figure 10. Interactions between **3** and Leu251, Val259, and Leu371 of LCK. The green lines indicate CH/π hydrogen bonds.

To summarize this section, the FMO results revealed that BMS-279700 **2** interacts with the LCK protein through not only hydrogen bonds but also through CH/O, NH/π, and CH/π hydrogen bonds and that this has enough interaction energy to be a candidate for the lead compound. We therefore tried to improve the binding ability of **2**, taking CH/π hydrogen bonds into further consideration.

2.4. Compound 3

2.4.1. *N*-(2-Chlorophenyl)-5-phenylimidazo[1,5-*a*]pyrazin-8-amine

In view of the results obtained by the FMO analysis of the above two complexes, we hypothesized that CH/O and CH/π hydrogen bonds play an important role in the binding of inhibitors with the LCK protein. Thus, *N*-(2-chlorophenyl)-5-phenylimidazo[1,5-*a*]pyrazin-8-amine (**3**) was designed and synthesized as a candidate inhibitor. First, we determined the crystal structure of **3** in complex with the LCK kinase domain. Next, FMO calculations were carried out to obtain information necessary for optimizing the structure of potential ligands.

Table 3 shows that **3** interacts with Thr#316 (−7.8 kcal/mol), Tyr#318 (−9.7 kcal/mol), and Met#319 (−9.7 kcal/mol). The binding mode of these three residues is similar to that of **2**.

In the crystal structure (Fig. 10), short CH/π contacts are shown between the imidazo-pyrazine moiety of **3** and the side chain groups of Val259 and Leu371. In agreement with this observation, the FMO calculations show that **3** interacts with Val#259 and Leu#371; their interaction energies are −2.0 and −4.3 kcal/mol, respectively. In contrast, the HF interaction energies involving these two residues are positive, suggesting that hydrogen bonds do not play a role. Although Leu251 interacts with the core-ring part of **1** and **2** via CH/π hydrogen bonds, in **3**, Leu251 is remote from the imidazo-pyrazine ring. In contrast, short CH/π contacts have been noted between the side chain of Leu251 and the phenyl ring at position 5 of the imidazo-pyrazine ring. The calculated interaction energy (−2.5 kcal/mol) is consistent with the crystal structure. The tricyclic ring in the core region of the inhibitor **2** is

Table 3
Interaction energies (in kcal/mol) between the LCK and compound **3**

	E_{MP2}[a]	E_{HF}[b]	ΔE_{MP2-HF}[c]
Met319	−9.7	−6.0	−3.7
Tyr318	−9.7	−6.1	−3.6
Thr316	−7.8	−3.1	−4.7
Glu288	−6.9	−4.7	−2.2
Lys273	−6.7	−2.3	−4.5
Gly252	−4.7	−3.7	−1.1
Leu371	−4.3	0.9	−5.2
Leu251	−2.5	0.5	−3.0
Lys269	−2.2	−2.2	0.0
Val259	−2.0	1.6	−3.6
Asp326	−2.0	−1.9	−0.1
Met319	−1.9	−0.5	−1.3
Val272	−1.8	−1.2	−0.6
Trp260	−1.8	−1.7	−0.2
Ile314	−1.7	−0.3	−1.4
Val301	−1.6	0.7	−2.3
Ala381	−1.6	−0.9	−0.6
Gly322	−1.5	−0.6	−0.9
Ser274	−1.2	−1.1	−0.1

[a] Interaction energy calculated at the MP2/6-31G level.
[b] Interaction energy calculated at the HF/6-31G level.
[c] $E_{MP2} - E_{HF}$.

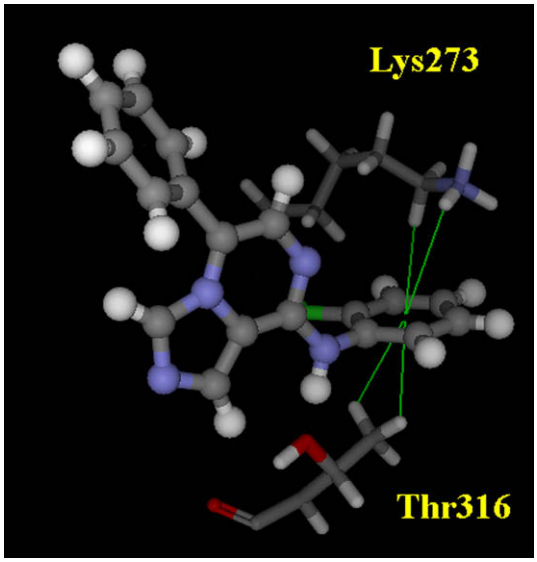

Figure 11. Interactions between **3** and Lys273 and Thr316 of LCK. The green lines indicate NH/π and CH/π hydrogen bonds.

converted to a bicyclic ring in **3**. Three amino acid residues (Val259, Leu371, and Leu251) interacting with **2** by CH/π hydrogen bonds are also involved in **3**.

Figure 11 shows short CH/π contacts between the benzene ring of **3** and the side chain of Lys273 and Thr316. In agreement with this observation, the interaction energies were calculated to be −6.7 kcal/mol for Lys273 and −7.8 kcal/mol for Thr316 (Table 3). The 2-chlorol-aniline part of **3** interacts with Lys273 through NH/π and CH/π hydrogen bonds; Thr316 interacts via hydrogen bonds and CH/π hydrogen bonds.[3,54–56]

To summarize, the FMO calculation shows that **3** interacts with the LCK protein through CH/O, NH/π, and CH/π hydrogen bonds. However, the inhibition value of **3** to the LCK protein remained modest (IC_{50} = 220 nM).

2.5. Compound 4

2.5.1. *N*-(2,6-Dimethylphenyl)-5-phenylimidazo[1,5-*a*]pyrazin-8-amine

In the previous section, we noted that the interaction of the LCK protein with the 2-chlorol-aniline part of **3** is stabilized by CH/π and NH/π hydrogen bonds. The substituent effects on the CH/π hydrogen bond have been measured in many studies using IR and NMR spectroscopy,[57,58] X-ray crystallography,[59,60] and ab initio calculations.[27,61,62] According to these papers, it was shown that an electron-donating substituent on the π-ring system favors the CH/π hydrogen bond. We therefore designed *N*-(2,6-dimethylphenyl)-5-phenylimidazo[1,5-*a*]pyrazin-8-amine **4** to improve the interactions.

The present FMO results agree well with the structure activity relationship (SAR) of **3** and **4** (Table 4). The difference in the interaction energies of Lys273 between **3** and **4** were −6.0 kcal/mol, which was the largest value among the amino acid residues in the protein. Since the side chain of Lys273 was located above the 2,6-dimethylphenyl ring of **4**, the enhanced activity of **4** was attributable to the NH/π and CH/π hydrogen bonds. In contrast, the difference in the interaction energies in Thr316 was small (−0.02 kcal/mol). The HF interaction energy decreased 1.2 kcal/mol from **3** to **4**, while the dispersion energy increased by −1.2 kcal/mol. This result may be attributable to the decrease in the acidity of NH in the aniline part of the candidate inhibitors and the increase of electron density in the benzene ring by the introduction of methyl groups at positions 2 and 6. The differences in the interaction energies involving other residues were insignificant in the cases of Met319 (0.13 kcal/mol), Tyr318 (0.89 kcal/mol), Leu371 (0.05 kcal/mol), Val259 (−0.6 kcal/mol), and Leu251 (0.02 kcal/mol). The interactions between **4** and the LCK protein were similar to **3** in the linker region and imidazo-pyrazine ring. In agreement with the statement by Snow et al., 2,6-disubstitutions might have stabilized the conformation of the inhibitor in the complex.[34] Consequently, **4** is highly potent as an inhibitor of the LCK protein (IC_{50} = 20 nM).

Table 4
Interaction energies (in kcal/mol) between the LCK and compound **4**

	E_{MP2}[a]	E_{HF}[b]	ΔE_{MP2-HF}[c]
Lys273	−12.7	−7.7	−5.0
Met319	−9.6	−5.9	−3.7
Tyr318	−8.8	−5.7	−3.1
Thr316	−7.8	−1.9	−5.9
Gly252	−5.8	−4.2	−1.6
Leu371	−4.3	0.5	−4.8
Glu288	−3.5	−0.7	−2.8
Ile315	−3.1	−1.9	−1.2
Val272	−2.9	−2.1	−0.8
Val259	−2.6	1.4	−4.0
Leu251	−2.4	0.9	−3.4
Val301	−1.8	0.7	−2.5
Met292	−1.7	−0.1	−1.6
Lys269	−1.7	−1.7	0.0
Ile314	−1.4	0.6	−2.0
Gly322	−1.4	−0.5	−0.8
Asp326	−1.3	−1.3	0.0
Phe383	−1.2	0.0	−1.2
Trp260	−1.1	−0.9	−0.3

[a] Interaction energy calculated at the MP2/6-31G level.
[b] Interaction energy calculated at the HF/6-31G level.
[c] $E_{MP2} - E_{HF}$.

3. Conclusions

The interaction energy was calculated by the ab initio FMO method for complexes between the LCK protein and four inhibitors (staurosporine **1**, BMS compound **2**, and compounds **3** and **4**). In the four complexes investigated, CH/π hydrogen bonds were found to play an important role in the binding of the protein to the inhibitors. In the complexes of every ligand, several CH/π hydrogen bonds were disclosed in the so-called adenine pocket. In **2**, **3**, and **4**, CH/π and NH/π hydrogen bonds were also observed in another pocket, which was not occupied by ATP. Additionally, CH/O hydrogen bonds have been shown to play a role in the linker region. According to the above findings, the aniline ring in **3** was substituted by 2,6-dimethyl in **4** to increase the potency for LCK kinase. Thus, a 10-fold increase in the potency was achieved for **4** (IC_{50} = 20 nM) over **3** (IC_{50} = 20 nM). We suggest that CH/π hydrogen bonds play an indispensable role in the recognition of the LCK protein with the ligand and the signal transduction system. The concept of CH/π hydrogen bonds is useful in the rational design of drugs.

4. Methods

4.1. Molecular modeling

The structure of LCK/**1**-complex was retrieved from the Protein Data Bank (PDB); the PDB code is 1qpj.[44] The crystal structures of LCK complexes with inhibitors **2**, **3**, and **4** were determined in our laboratory (PDB codes 2zm4, 2zm1, and 2zob, respectively). The resolution of the crystallographic determinations of the protein/ligand complexes were 2.2, 2.7, 2.1, and 2.6 Å for **1**, **2**, **3**, and **4**, respectively. Hydrogen atoms were generated by using the molecular graphic software Quanta 2000 (Accelrys, Inc., San Diego, CA). We assumed that the N-termini of the lysine and arginine side chains were protonated, while the C-termini of aspartic and glutaminic side chains were deprotonated. The amino groups of inhibitors **1** and **2** were not protonated. The CHARMm force field implemented in Quanta 2000 was used at the minimization steps. The protein structures were optimized by the steepest descent (SD) method at dielectric constant $\varepsilon = 4R$. The optimization was performed stepwise. At the first step, the structures were minimized under the condition that the non-hydrogen atoms were constrained. Next, the protein backbone atoms were constrained. At the final step, all atoms were minimized with the harmonic atom constraint. The force constants of the harmonic atom constraint gradually decreased from 100.0 to 10.0, and then to 1.0.

4.2. FMO method

First, a molecule or a molecular cluster was divided into M fragments (monomers) as shown in Figure 12. Then, ab initio calculations were carried out, repeatedly, on the fragments under the electrostatic potential from the surrounding $(M-1)$ monomers V^I, until all the monomer densities become self-consistent. Second,

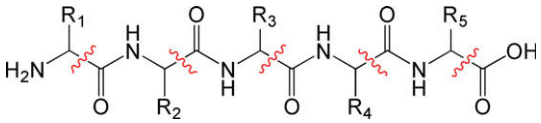

Figure 12. Fragmentation of molecules; proteins were divided into each amino acid residues.

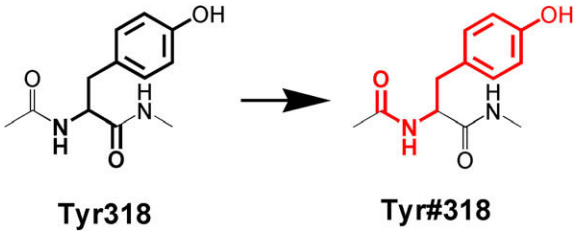

Figure 13. Amino acid residues renumbered based on the FMO fragment rule.

the equations for the dimers were solved under the influence of the electrostatic potential from the neighboring $(M-2)$ monomers V^{IJ}. Finally, the total energy of the system E is calculated in Eq. 1 by using the total energies of the monomer E^{I} and dimer E^{IJ}.

$$E = \sum_{I>J}^{M} E_{IJ} - (M-2)\sum_{I}^{M} E_{I} \tag{1}$$

The internal fragments interaction energy (IFIE) in the FMO calculations is defined as in Eq. 2.

$$\Delta E_{IJ} = (E'_{IJ} - E'_{I} - E'_{J}) + Tr(\Delta P^{IJ} V^{IJ}) \tag{2}$$

where P^{IJ} is a difference density matrix, V^{IJ} is the environmental electrostatic potential for dimmer IJ, and E'_{I} and E'_{IJ} are the monomer and dimmer energy, respectively, without an environmental electrostatic potential.

In the present study, the proteins were divided at individual amino acid residues because our aim was to investigate the intermolecular interactions between the LCK protein and the inhibitors based on an amino acid residue units. Note that fragmented residues do not exactly correspond to amino acid residues because the fragmentations in the FMO calculations were performed between the Cα atom and the main chain carbonyl group. Therefore, the main chain carbonyl group of the ith residue was assigned to the $(i+1)$th residue fragment. In the following discussion, we refer to fragmented amino acid residues using the residue name and its position from the N-terminus (#). For example, Figure 13 shows that Tyr#318 consists of the carbonyl group of Glu317 through Tyr318, but does not include the carbonyl group of Tyr318.

Single-point energy calculations were performed by the HF and MP2 methods using the 6-31G basis set (FMO-HF/6-31G, FMO-MP2/6-31G). All of the FMO calculations were carried out using the ABINIT-MP program.[63] The calculations were done on Pentium 4 3.4-GHz clusters (20 CPUs). The CPU time took about 52 h for the LCK/**4** complex (4433 atoms, 24,524 basis functions).

Acknowledgments

We thank Dr. Tatsuya Nakano (National Institute of Health Sciences) for his valuable advice in interpreting the FMO results and encouragement, Dr. Motohiro Nishio (The CHPI Institute) for discussions and reading the manuscript, Prof. Kazuo Kitaura (Kyoto University) for his valuable advice and suggestions in performing the FMO calculations, and T.O. would acknowledge the professional technical supports by the "Revolutionary Simulation Software" (RSS21) project of the Ministry of Education, Culture, Sports, Science, and Technology.

References and notes

1. Nishio, M.; Hirota, M.; Umezawa, Y. *The CH/π Interaction. Evidence, Nature, and Consequences*. New York: Wiley-VCH, 1998.
2. Tewari, A. K.; Dubey, R. *Bioorg. Med. Chem.* **2008**, *16*, 126.
3. Umezawa, Y.; Nishio, M. *Bioorg. Med. Chem.* **1998**, *6*, 493.
4. Toth, G.; Bowers, S. G.; Truong, A. P.; Probst, G. *Curr. Pharm. Des.* **2007**, *13*, 3476.
5. Pierce, A. C.; Sandretto, K. L.; Bemis, G. W. *Proteins Struct. Funct. Bioinf.* **2002**, *49*, 567.
6. Pierce, A. C.; Haar, E.; Binch, H. M. *J. Med. Chem.* **2005**, *48*, 1278.
7. Umezawa, Y.; Nishio, M. *Biopolymers* **2005**, *79*, 248.
8. Nakagawa, Y.; Irie, K.; Yanagita, R. C.; Ohigashi, H.; Tsuda, K. *J. Am. Chem. Soc.* **2005**, *127*, 5746.
9. Kitaura, K.; Morokuma, K. *Int. J. Quantum Chem.* **1976**, *10*, 325.
10. Hayes, I. C.; Stone, A. *J. Mol. Phys.* **1984**, *53*, 83.
11. Takahashi, O.; Kohno, Y.; Iwasaki, S.; Saito, K.; Iwaoka, M.; Tomoda, S.; Umezawa, Y.; Tsuboyama, S.; Nishio, M. *Bull. Chem. Soc. Jpn.* **2001**, *74*, 2421.
12. Spiwok, V.; Lipovova, P.; Skalova, T.; Buchtelova, E.; Hasek, J.; Kralova, B. *Carbohydr. Res.* **2004**, *339*, 2275.
13. Tsuzuki, S.; Uchimaru, T. *Curr. Org. Chem.* **2006**, *10*, 745.
14. Kitaura, K.; Sawai, T.; Asada, T.; Nakano, T.; Uebayasi, M. *Chem. Phys. Lett.* **1999**, *312*, 319.
15. Kitaura, K.; Ikeo, E.; Asada, T.; Nakano, T.; Uebayasi, M. *Chem. Phys. Lett.* **1999**, *313*, 701.
16. Nakano, T.; Kaminuma, T.; Sato, T.; Akiyama, Y.; Uebayasi, M.; Kitaura, K. *Chem. Phys. Lett.* **2000**, *318*, 614.
17. Nakano, T.; Kaminuma, T.; Sato, T.; Fukuzawa, K.; Akiyama, Y.; Uebayasi, M.; Kitaura, K. *Chem. Phys. Lett.* **2002**, *351*, 475.
18. Fedorov, D. G.; Kitaura, K. In *Modern Methods for Theoretical Physical Chemistry of Biopolymers*; Starikov, E. B.; Lewis, J. P.; Tanaka, S., Eds.; Elsevier, 2006, Chapter 1, pp 3–38.
19. Nakano, T.; Mochizuki, Y.; Fukuzawa, K.; Amari, S.; Tanaka, S. In *Modern Methods for Theoretical Physical Chemistry of Biopolymers*; Starikov, E. B.; Lewis, J. P.; Tanaka, S., Eds.; Elsevier, 2006, Chapter 2, pp 39–52.
20. Mochizuki, Y.; Nakano, T.; Koikegami, S.; Tanimori, S.; Abe, Y.; Nagashima, U.; Kitaura, K. *Theor. Chem. Acc.* **2004**, *112*, 442.
21. Mochizuki, Y.; Koikegami, S.; Nakano, T.; Amari, S.; Kitaura, K. *Chem. Phys. Lett.* **2004**, *396*, 473.
22. Fedorov, D. G.; Kitaura, K. *J. Chem. Phys.* **2004**, *121*, 2483.
23. Fukuzawa, K.; Mochizuki, Y.; Tanaka, S.; Kitaura, K.; Nakano, T. *J. Phys. Chem. B* **2006**, *110*, 16102.
24. Fukuzawa, K.; Komeiji, Y.; Mochizuki, Y.; Kato, A.; Nakano, T.; Tanaka, S. *J. Comput. Chem.* **2006**, *27*, 948.
25. Nakanishi, I.; Fedorov, D. G.; Kitaura, K. *Proteins Struct. Funct. Bioinf.* **2007**, *68*, 145.
26. Sakaki, S.; Kato, K.; Miyazaki, T.; Musashi, Y.; Ohkubo, K.; Ihara, H.; Hirayama, C. *J. Chem. Soc., Faraday Trans.* **1993**, *89*, 659.
27. Ran, J.; Wong, M. W. *J. Phys. Chem. A* **2006**, *110*, 9702.
28. Ozawa, T.; Okazaki, K. *J. Comput. Chem.* **2008**, *29*, 2656.
29. Susva, M.; Missbach, M.; Green, J. *Trends Pharmacol. Sci.* **2000**, *21*, 489.
30. Marth, J. D.; Lewis, D. B.; Cooke, M. P.; Mellins, E. D.; Gearn, M. E.; Samelson, L. E.; Wilson, C. B.; Miller, A. D.; Perlmutter, R. M. *J. Immunol.* **1989**, *142*, 2430.
31. Palacios, E. H.; Weiss, A. *Oncogene* **2004**, *23*, 7990.
32. Hanke, J. H.; Gardner, J. P.; Dow, R. L.; Changelian, P. S.; William, H.; Brissette, W. H.; Weringer, E. J.; Pollok, B. A.; Connelly, P. A. *J. Biol. Chem.* **1996**, *271*, 695.
33. Trevillyan1, J. M.; Chiou, G. Gr.; Ballaron, S.; Tang, Q. M.; Buko, A.; Sheets, M. P.; Smith, M. L.; Putman, C. B.; Wiedeman, P.; Tu, N.; Madar, D.; Smith, H. T.; Gubbins, E. J.; Warrior, U. P.; Yung-Wu, J. *Arch. Biochem. Biophys.* **1999**, *364*, 19.
34. Snow, R. J.; Cardozo, M. G.; Morwick, T. M.; Busacca, C. A.; Dong, Y.; Eckner, R. J.; Jacober, S.; Jakes, S.; Kapadia, S.; Lukas, S.; Panzenbeck, M.; Peet, G. W.; Peterson, J. D.; Prokopowicz, A. S.; Sellati, R.; Tolbert, R. M.; Tschantz, M. A.; Moss, N. *J. Med. Chem.* **2002**, *45*, 3394.
35. Goldberg, D. R.; Butz, T.; Cardozo, M. G.; Eckner, R. J.; Hammach, A.; Huang, J.; Jakes, S.; Kapadia, S.; Kashem, M.; Lukas, S.; Morwick, T. M.; Panzenbeck, M.; Patel, U.; Pav, S.; Peet, G. W.; Peterson, J. D.; Prokopowicz, A. S.; Snow, R. J.; Sellati, R.; Takahashi, H.; Tan, J.; Tschantz, M. A.; Wang, X.; Wang, Y.; Wolak, J.; Xiong, P.; Moss, N. *J. Med. Chem.* **2003**, *46*, 1337.
36. Chen, P.; Norris, D.; Iwanowicz, E. J.; Spergel, S. H.; Lin, J.; Gu, H. H.; Shen, Z.; Wityak, J.; Lin, T. A.; Pang, S.; Fex, H.; Pitt, S.; Shen, D. R.; Doweyko, A. M.; Bassolino, D. A.; Roberge, J. Y.; Poss, M. A.; Chen, B.; Schieven, G. L.; Barrish, J. C. *Bioorg. Med. Chem. Lett.* **2002**, *12*, 1361.
37. Chen, P.; Iwanowicz, E. J.; Norris, D.; Gu, H. H.; Lin, J.; Moquin, R. V.; Das, J.; Wityak, J.; Spergel, S. H.; Fex, H.; Pang, S.; Pitt, S.; Shen, D. R.; Schieven, G. L.; Barrish, J. C. *Bioorg. Med. Chem. Lett.* **2002**, *12*, 3153.
38. Das, J.; Lin, J.; Moquin, R. V.; Shen, Z.; Spergel, S. H.; Wityak, J.; Doweyko, A. M.; DeFex, H. F.; Fang, Q.; Pang, S.; Pitt, S.; Shen, D. R.; Schieven, G. L.; Barrish, J. C. *Bioorg. Med. Chem. Lett.* **2003**, *13*, 2145.
39. Chen, P.; Norris, D.; Das, J.; Spergel, S. H.; Wityak, J.; Leith, L.; Zhao, R.; Chen, B.; Pitt, S.; Pang, S.; Shen, D. R.; Zhang, R.; De Fex, H. F.; Doweyko, A. M.; McIntyre, K. W.; Shuster, D. J.; Behnia, K.; Schieven, G. L.; Barrish, J. C. *Bioorg. Med. Chem. Lett.* **2004**, *14*, 6061.

40. Chen, P.; Doweyko, A. M.; Norris, D.; Gu, H. H.; Spergel, S. H.; Das, J.; Moquin, R. V.; Lin, J.; Wityak, J.; Iwanowicz, E. J.; McIntyre, K. W.; Shuster, D. J.; Behnia, K.; Chong, S.; De Fex, H. F.; Pang, S.; Pitt, S.; Shen, D. R.; Thrall, S.; Stanley, P.; Kocy, O. R.; Witmer, M. R.; Kanner, S. B.; Schieven, G. L.; Barrish, J. C. *J. Med. Chem.* **2004**, *47*, 4517.
41. Arnold, L. D.; Calderwood, D. J.; Dixon, R. W.; Johnston, D. N.; Kamens, J. S.; Munschauer, R.; Rafferty, P.; Ratnofsky, S. E. *Bioorg. Med. Chem. Lett.* **2000**, *10*, 2167.
42. Burchat, A. F.; Calderwood, D. J.; Friedman, M. M.; Hirst, G. C.; Rafferty, P.; Ritter, K.; Skinner, B. S. *Bioorg. Med. Chem. Lett.* **2002**, *12*, 1687.
43. Borhani, D. W.; Calderwood, D. J.; Friedman, M. M.; Hirst, G. C.; Leung, K. W.; McRae, B.; Ratnofsky, S.; Ritter, K.; Waegell, W. *Bioorg. Med. Chem. Lett.* **2004**, *14*, 2613.
44. Zhu, X.; Kim, J. L.; Newcomb, J. R.; Rose, P. E.; Stover, D. R.; Toledo, L. M.; Zhao, H.; Morgenstern, K. A. *Structure* **1999**, *7*, 651.
45. Chery, M.; Williiams, D. H. *Curr. Med. Chem.* **2004**, *11*, 663.
46. Mukaiyama, H.; Nishimura, T.; Kobayashi, S.; Ozawa, T.; Kamada, N.; Komatsu, Y.; Kikuchi, S.; Oonota, H.; Kusama, H. *Bioorg. Med. Chem.* **2007**, *15*, 868.
47. Ishikawa, T.; Mochizuki, Y.; Amari, S.; Nakano, T.; Tokiwa, H.; Tanaka, S.; Tanaka, K. *Theor. Chem. Acc.* **2007**, *118*, 937.
48. Grimme, S. *J. Chem. Phys.* **2003**, *118*, 9095.
49. Ishikawa, T.; Mochizuki, Y.; Amari, S.; Nakano, T.; Tanaka, S.; Tanaka, K. *Chem. Phys. Lett.* **2008**, *463*, 189.
50. Ghose, A. K.; Herbertz, T.; Pippin, D. A.; Salvino, J. M.; Mallamo, J. P. *J. Med. Chem.* **2008**, *51*, 5149.
51. Lipinski, C. A.; Lombardo, F.; Dominy, B. W. *Adv. Drug Delivery Rev.* **2001**, *46*, 3.
52. Congreve, M.; Carr, R.; Murray, C. *Drug Discovery Today* **2003**, *8*, 876.
53. Sarkhel, S.; Desiraju, G. R. *Proteins Struct. Funct. Bioinf.* **2004**, *54*, 247.
54. Ref. 1, pp 189–194.
55. Chakrabarti, P.; Samanta, U. *J. Mol. Biol.* **1995**, *251*, 9.
56. Harigai, M.; Kataoka, M.; Imamoto, Y. *J. Am. Chem. Soc.* **2006**, *128*, 10646.
57. Ehama, R.; Tsushima, M.; Yuzuri, T.; Suezawa, H.; Sakakibara, K.; Hirota, M. *Bull. Chem. Soc. Jpn.* **1993**, *66*, 814.
58. Suezawa, H.; Mori, A.; Sato, M.; Ehama, R.; Akai, I.; Sakakibara, K.; Hirota, M.; Nishio, M.; Kodama, Y. *J. Phys. Org. Chem.* **1993**, *6*, 399.
59. Nishio, M. *Cryst. Eng. Commun.* **2004**, *6*, 130.
60. Chowdhury, S. K.; Joshi, V. S.; Samuel, A. G.; Puranik, V. G.; Tavale, S. S.; Sarkar, A. *Organometallics* **1994**, *13*, 4092.
61. Lee, E. C.; Hong, B. H.; Lee, J. Y.; Kim, J. C.; Kim, D.; Kim, Y.; Tarakesh, P. *J. Am. Chem. Soc.* **2005**, *127*, 4530.
62. Gil, A.; Branchadell, V.; Oliva, A. *J. Phys. Chem. B* **2007**, *111*, 9372.
63. ABINIT-MP. Available at http://www.ciss.iis.u-tokyo.ac.jp/rss21/result/download/index.php#download_2.